DNA Radiosensitization

International Edition: DOI: 10.1002/anie.201603464
German Edition: DOI: 10.1002/ange.201603464

Sensitizing DNA Towards Low-Energy Electrons with 2-Fluoroadenine

*Jenny Rackwitz, Janina Kopyra, Iwona Dąbkowska, Kenny Ebel, MiloŠ Lj. Ranković, Aleksandar R. Milosavljević, and Ilko Bald**

Abstract: *2-Fluoroadenine (^{2F}A) is a therapeutic agent, which is suggested for application in cancer radiotherapy. The molecular mechanism of DNA radiation damage can be ascribed to a significant extent to the action of low-energy (< 20 eV) electrons (LEEs), which damage DNA by dissociative electron attachment. LEE induced reactions in ^{2F}A are characterized both isolated in the gas phase and in the condensed phase when it is incorporated into DNA. Information about negative ion resonances and anion-mediated fragmentation reactions is combined with an absolute quantification of DNA strand breaks in ^{2F}A-containing oligonucleotides upon irradiation with LEEs. The incorporation of ^{2F}A into DNA results in an enhanced strand breakage. The strand-break cross sections are clearly energy dependent, whereas the strand-break enhancements by ^{2F}A at 5.5, 10, and 15 eV are very similar. Thus, ^{2F}A can be considered an effective radiosensitizer operative at a wide range of electron energies.*

Radiation therapy using high-energy photons, electrons, or ions belongs to the most important methods used to treat cancer. As was shown in recent years, the radiation damage induced by the high-energy primary radiation is mostly due to the effect of low-energy secondary particles generated along the ionization track.[1,2] Low-energy electrons (LEEs) belong to the most important intermediates, since they are produced in significant quantities[2,3] and can directly attach to DNA and other biomolecules to form transient negative ions, which are unstable towards dissociation.[4] In DNA, dissociative electron attachment (DEA) can result in effective single and double strand breaks.[5,6]

In radiation therapy, radiosensitizers are used as therapeutics to enhance the radiation damage to the tumor tissue.[7] On a physicochemical level the radiosensitization can be ascribed to an enhanced reactivity towards LEEs.[8] The most important administered drugs in chemoradiotherapy are cisplatin and its derivatives,[9] 5-fluorouracil[10], and gemcitabine,[11] whose reactivities towards LEEs have been clearly shown.

Fludarabine, a nucleoside containing 2-fluoroadenine (^{2F}A), is an established chemotherapeutic,[12] but is also considered as a potential radiosensitizer.[13] Herein, we analyze the reactivity of ^{2F}A towards low-energy electrons. We investigate the change of the absolute strand-break cross section when ^{2F}A is incorporated into an oligonucleotide to replace adenine (A) and analyze the observations in terms of negative ion resonances revealed by DEA spectroscopy in the gas phase.

The response of single model compounds of DNA to LEEs has been studied in great detail,[1,14] but thus far it was unclear whether such gas-phase results can be transferred to the condensed phase and the situation in an oligonucleotide; that is, how the anion resonances observed in gas-phase experiments can be connected to an actual DNA strand-break process. In the present study we compare the gas phase results to absolute strand-break cross sections obtained at three different electron energies using our recently established DNA origami-based technique.[15,16] In this way we accurately quantify the effect of the incorporation of radiosensitizers into oligonucleotides and, hence, can assess the quality of potential radiosensitizers.

Figure 1a shows the general approach for the determination of the absolute cross sections for DNA strand breakage induced by LEEs (detailed experimental procedures can be found in Ref. [15–17] and in the Supporting Information). Two different biotinylated target sequences are attached to the DNA origami platforms, which are immobilized on Si/SiO_2 substrates. After electron irradiation, the remaining intact oligonucleotides are visualized by atomic force microscopy (AFM) with streptavidin (SAv). In Figure 1b, a non-irradiated control sample is shown, and in the expanded area, the two different positions of two target sequences (central and side positions, respectively) can be clearly distinguished. As the target sequence we chose 5′-d(TT(ATA)$_3$TT) (side position) and 5′-d(TT(^{2F}AT^{2F}A)TT) (central position) to directly compare the strand-break yields of a non-modified DNA sequence and a DNA sequence modified with ^{2F}A. It was demonstrated previously that 5′-d(TT(ATA)$_3$TT) is particularly sensitive to damage by LEEs.[15] For comparison we have also determined strand-break cross sections upon

[*] J. Rackwitz, K. Ebel, Prof. Dr. I. Bald
Institute of Chemistry—Physical Chemistry, University of Potsdam
Karl-Liebknecht-Str. 24–25, 14476 Potsdam (Germany)
E-mail: ilko.bald@uni-potsdam.de
Dr. J. Kopyra
Faculty of Sciences, Siedlce University
3 Maja 54, 08-110 Siedlce (Poland)
Dr. I. Dąbkowska
Department of Chemistry, University of Gdańsk
80-952 Gdańsk (Poland)
M. Ranković, Prof. Dr. A. R. Milosavljević
Institute of Physics Belgrade, University of Belgrade
Pregrevica 118, 11080 Belgrade (Serbia)
Prof. Dr. A. R. Milosavljević
SOLEIL, l'Orme des Merisiers, St. Aubin
BP48, 91192, Gif sur Yvette Cedex (France)
Prof. Dr. I. Bald
Department 1—Analytical Chemistry and Reference Materials
BAM Federal Institute for Materials Research and Testing
Richard-Willstätter Str. 11, 12489 Berlin (Germany)

Supporting information for this article can be found under: http://dx.doi.org/10.1002/anie.201603464.

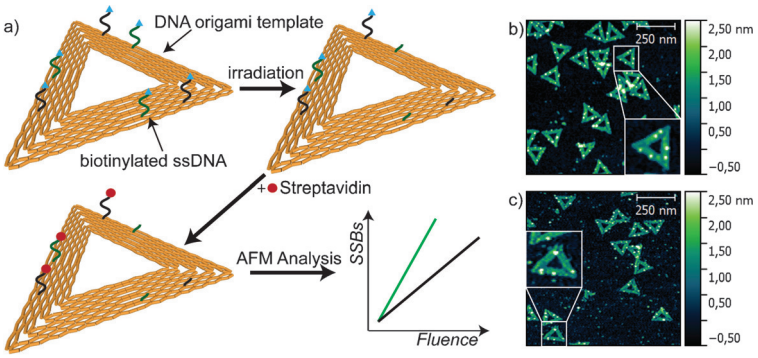

Figure 1. a) Experimental procedure to determine the absolute cross sections of DNA strand breakage. b), c) Examples of AFM images of b) a non-irradiated control sample and c) a sample irradiated with 10 eV electrons for 60 s at 5.5 nA.

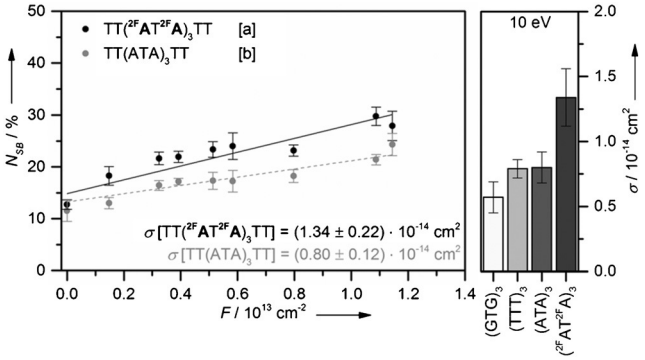

Figure 2. Left: Fluence dependence of strand breakage of the two oligonucleotide sequences 5′-d(TT(^{2F}AT^{2F}A)$_3$TT) (sequence a) and 5′-d(TT(ATA)$_3$TT) (sequence b). Irradiation was performed at 10 eV electron energy. Right: Absolute strand-break cross sections σ obtained from the linear fit of the fluence dependence of strand breakage in different sequences. For clarity only the central sequence is shown.

10 eV electron irradiation for the sequences 5′-d(TT(GTG)$_3$TT) and T$_{12}$ (Figure 2 Right and Figure S1 in the Supporting Information). Figure 1c shows a typical AFM image after LEE irradiation. From the AFM images the relative number of strand breaks (N_{SB}) is determined for various electron fluences (see the Supporting Information). The fluence is chosen to be small enough that no saturation of N_{SB} is reached as it was observed in earlier experiments.[15] From the slope of the linear fit of the exposure response curve the absolute cross sections for strand breakage for the two target sequences are obtained as shown in Figure 2 for 10 eV electrons. 10 eV was chosen because in previous experiments using plasmid DNA the highest strand break yield was found at this energy.[5,18] For the non-modified DNA sequence 5′-d(TT(ATA)$_3$TT) we find a strand-break cross section of $\sigma = (0.80 \pm 0.12) \times 10^{-14}$ cm^2, whereas for the modified sequence 5′-d(TT(^{2F}AT^{2F}A)TT) we obtain a value of $\sigma = (1.34 \pm 0.22) \times 10^{-14}$ cm^2. This results in a strand-break enhancement factor (EF) of 1.7 ± 0.5. This value corresponds to the highest EF found in previous studies of BrU-modified oligonucleotides.[16] Very recently, an EF of approximately 1.5 was reported for SSBs in plasmid DNA mixed with cisplatin and derivatives irradiated with 10 eV electrons.[19] This indicates that ^{2F}A is an effective radiosensitizer in terms of enhancement of strand breakage. The modified sequence 5′-d(TT(^{2F}AT^{2F}A)TT) also shows a higher sensitivity towards 10 eV electrons compared to the sequences 5′-d(TT(GTG)$_3$TT) and 5′-dT$_{12}$, which have strand break cross sections of $(0.57 \pm 0.12) \times 10^{-14}$ cm^2 and $(0.79 \pm 0.07) \times 10^{-14}$ cm^2, respectively (Figure 2).

The absolute cross sections for strand breakage are in the same order of magnitude as the effective and absolute cross sections found in earlier studies for strand breakage in plasmid DNA ($(2.7 \pm 1.8) \times 10^{-14}$ cm^2 and $(3.8 \pm 1.2) \times 10^{-14}$ cm^2, respectively).[20]

To obtain more information on the involved negative ion resonances and specific DEA reactions, we have studied DEA to ^{2F}A in the gas phase using a crossed electron-molecular beam experimental setup to record fragment anion yields as a function of electron energy (see the Supporting Information for more detailed information on the experimental procedure). The anion yield curves of selected fragmentation products are shown in Figure 3.

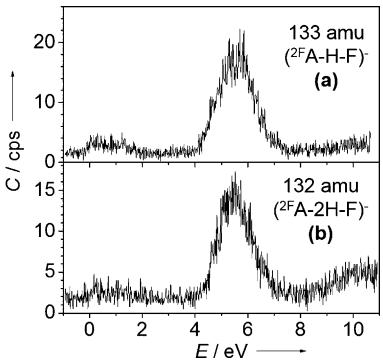

Figure 3. Ion count rate C for fragment anions detected at m/z 133 and 132 resulting from electron attachment to ^{2F}A. These fragmentation products are mainly observed within broad resonances at 4.5–7.0 eV. E = electron energy.

In total, fragment ions have been observed within resonant features located at 0.3–3 eV, 4–7 eV, and weakly around 10 eV (see below). Two fragment anions at m/z 133 ($(^{2F}A-H-F)^-$) and m/z 132 ($(^{2F}A-2H-F)^-$) have been observed, both within a broad resonance centered at 5.5 eV (Figure 3a,b). The fragment anion at m/z 132 appears additionally around 10 eV with a lower intensity. The fragment anions are formed by the loss of F and one or two H atoms, respectively, from the transient negative ion $^{2F}A^{\#-}$. The same m/z ratios have previously been observed in A, at 7.0 and 10.5 eV for the loss of two H atoms and at 6.5 and 10.9 eV for the loss of three H atoms.[21] Due to the presence of F in ^{2F}A, the negative-ion states of ^{2F}A are shifted to lower energies compared to A resulting in lower vertical attachment energies. The ion yield curves in Figure 3 clearly show the pronounced resonance around 5.5 eV and only a weak signal around 10 eV. This situation is in contrast to the ion yield

curves obtained for the same m/z ratios from A.[21] There, a clear signal at 10.5 eV was observed at m/z 133, which is even more dominant at m/z 132. Both resonances are assigned to a core-excited resonance. The formation of the m/z 133 and m/z 132 ions can also be accompanied by the formation of neutral HF, which has a high binding energy and can then thermodynamically drive the reaction. Indeed, it is frequently observed that the formation of fragment anions in the case of halo-nucleobases is driven by the formation of a neutral stable molecule of a halogen acid. This has been recently reported for 5-chlorouracil, 6-chlorouracil[22], and ^{2Cl}A.[23] In contrast, for 5-bromouracil (^{5Br}U) only the loss of the Br atom resulting in $(^{5Br}U-Br)^-$ was observed.[24] This can be easily attributed to the difference of the binding energy of H–X (X = F, Cl or Br), which decreases substantially from HF (5.9 eV) to HCl (4.5 eV) and HBr (3.8 eV).[25]

To test whether the anion resonance observed in the gas phase at 5.5 eV also leads to higher strand-break cross sections, a further condensed-phase experiment has been performed at 5.5 eV, which corresponds to the maximum of the resonance shown in Figure 3.

As shown in Figure 4, both sequences 5′-d(TT(ATA)$_3$TT) and 5′-d(TT(^{2F}AT^{2F}A)$_3$TT) indeed have a higher strand-break cross section at 5.5 eV than at 10 eV indicating a higher sensitivity of both sequences towards 5.5 eV electrons. However, the EF is again 1.6 ± 0.1 at 5.5 eV, which is the same (within the error bars) as that determined for 10 eV. In DEA to gas-phase ^{2F}A, the anion fragment $(^{2F}A-2H-F)^-$ appears at 5.5 eV and with lower intensity at 10 eV. This correlates well with the observed strand break cross sections. In DEA to A, the anion fragment $(A-2H)^-$ and a number of smaller fragment anions are formed at 5.0–6.0 eV and around 10 eV. The present results indicate that the LEE-induced strand breakage is particularly effective using the resonances at around 5.5 eV. This is also in accordance with recent experiments using plasmid DNA, in which the maximum strand breakage was found at 5.5 eV.[26] Additionally, we have determined strand-break cross sections at 15 eV for the same sequences (Figure 4 and Figure S2 in the Supporting Information), which are clearly lower than those at 10 eV. Nevertheless, the enhancement is the same within the error of the experiment (EF = 1.7 ± 0.9). The EF accounts for the more efficient decomposition of ^{2F}A compared to A within the oligonucleotide, which is true for each electron energy considered herein.

The discussion above is focused on the electron-energy regime > 5 eV. However, it should be noted that the most intense ion observed in DEA to ^{2F}A is the dehydrogenated molecular anion [Eq. (1)]:

$$^{2F}A + e^- \rightarrow {}^{2F}A^{\#-} \rightarrow (^{2F}A-H)^-(m/z\ 152) + H \quad (1)$$

The corresponding ion yield curve is shown in Figure 5a revealing a broad signal at 0.3–3.5 eV, which is composed of at least three resonances located at 0.8, 1.29, and 2.0 eV. At these low electron energies, the extra electron occupies a formerly empty molecular orbital without changing the initial electron configuration. Since the potential energy curve of such MOs is typically repulsive, the electron must be captured in a metastable state through a centrifugal energy

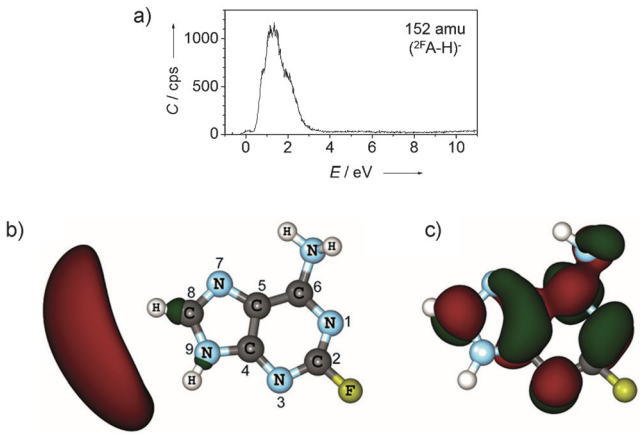

Figure 5. a) Ion count rate C for the fragment anion detected at m/z 152 within the energy regime of 0.3–3.5 eV resulting from electron attachment to ^{2F}A. b), c) Results of ab initio calculations of the anion of ^{2F}A. b) Dipole-bound anion state of ^{2F}A (MP2/CCSD(T)) showing also the molecular structure and the atom labeling of ^{2F}A, and c) the valence-bound anion of ^{2F}A (MP2).

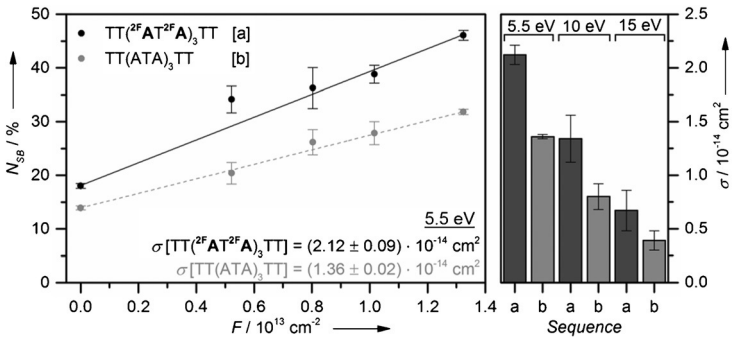

Figure 4. Left: Fluence dependence of the strand breakage of the two oligonucleotide sequences 5′-d(TT(^{2F}AT^{2F}A)$_3$TT) (sequence a) and 5′-d(TT-(ATA)$_3$TT) (sequence b). Irradiation was performed at 5.5 eV electron energy. Right: Comparison of the absolute strand-break cross sections σ obtained from the linear fit of the fluence dependence of strand breakage from 10 and 5.5 eV.

barrier (denoted here as $^{2F}A^{\#-}$).[27] A dehydrogenated parent ion was previously also observed in DEA to adenine (A) and 2-chloroadenine (^{2Cl}A) within several overlapping resonances between approximately 0.7 and 2.2 eV.[21,23,28,29] By using different methylated A derivatives, the resonances below 1.5 eV were assigned to an H loss from N9 (see Figure 5b a for the typical atom labelling in purine bases).[28] In both A and ^{2Cl}A the lowest energy resonances were assigned to vibrational Feshbach resonances (VFRs), whereas the signals between 1.1 and 2.2 eV were assigned to π* resonances.[23,28]

Taking the previous measurements on A and ^{2Cl}A into account, the 0.8 eV signal in the ion yield curve of $(^{2F}A-H)^-$ is assigned to a VFR, and the signals at 1.29 eV and 2.0 eV are assigned to π* resonances.

Compared to A, the resonance positions are slightly shifted to lower energies in ^{2F}A owing to the presence of the F atom. In ^{2F}A, the H abstraction can take place from N9, from the NH_2 group, or from C8. Based on the previous findings on A[28] and ^{2Cl}A,[23] the H loss below 2.0 eV is ascribed to a cleavage of the N9–H bond.

This is supported by ab initio calculations that we have performed at the DFT/B3LYP, MP2 and MP2/CCSD(T) levels of theory. The calculations predict metastable molecular valence-bound anions of ^{2F}A, which are adiabatically unbound with an electron affinity of −0.71 eV (MP2) and −0.67 eV (CCSD(T)), respectively. The MO representation of the valence bound anion (MP2) is shown in Figure 5c. However, the calculations indicate that ^{2F}A possesses a very high dipole moment (4.6 Debye), suggesting that an excess electron may be bound by the dipole force.[30] Indeed, adding extra diffuse functions to the aug-cc-pVDZ basis set allows us to render the dipole-bound anion state (DBS) stable (at Koopman's theory level). However, only CCSD(T) correction to the electron energy leads to positive values of the adiabatic electron affinity (0.02 eV). The DFT calculations predict only a geometrically stable DBS with an electron affinity of −0.24 eV. In both DBS anionic states (MP2/CCSD(T) and DFT), an extra electron localizes close to the N9–H bond in ^{2F}A, (see Figure 5b). This is most likely the precursor state for the H loss from $^{2F}A^-$, in agreement with previous findings on A and ^{2Cl}A.[23,28] In the present case, the energy thresholds for hydrogen loss from $^{2F}A^-$ from N9, C8, and N6 are 0.83, 1.90, and 3.08 eV, respectively (determined at DFT level), corresponding well to the broad feature on the DEA spectrum in Figure 5a. In conclusion, the lowest energy signals (peaking at 0.8 eV) are tentatively assigned to H loss from N9 most likely through a DBS, whereas the signals peaking at 1.29 and 2.0 eV are most likely due to π* valence states.

In addition to the fragment anions shown in Figures 3 and 5, we have also observed the smaller fragments FCN_2^- (at 0.55 eV), FCN^- (at 0.07 eV), and CN^- (at 1.61 eV and weakly around 6.3 eV), which are shown in Figure S1 in the Supporting Information. FCN^- is formed with considerable intensity and could therefore represent an important precursor for strand breakage induced by very low-energy electrons close to zero eV.

In conclusion, the present gas- and condensed-phase experiments indicate that ^{2F}A is an efficient radiosensitizer as a result of its increased reactivity towards LEEs. The condensed-phase experiments have shown a pronounced energy dependence of strand-break cross sections. The anion resonances observed at 5.5 eV in the gas phase are very likely the precursors of the strand break process observed in oligonucleotides in the condensed phase. Remarkably, the strand-break enhancement factor is 1.6–1.7 at all investigated energies, that is, 5.5, 10, and 15 eV. It needs to be explored in further experiments whether the strand-break cross sections follow a similar resonant profile as suggested by the gas-phase DEA data by recording a detailed energy dependence of the strand break cross section. In the future, we will extend our study to double-stranded DNA to explore the effect of ^{2F}A on double-strand breaks. This physicochemical insight into the mechanism of radiosensitization supports the use of ^{2F}A as a radiosensitizer in tumor radiation therapy.

Acknowledgements

This research was supported by the Federal Institute for Materials Research and Testing (BAM), by the Polish Ministry of Science and Higher Education, a Marie Curie FP7 Integration Grant within the 7th European Union Framework Programme, by the Deutsche Forschungsgemeinschaft (DFG) and the University of Potsdam. J.R. acknowledges a travel grant to Siedlce University, Siedlce (Poland) from the European Union via the COST Action MP1002 (Nano-IBCT). I.D. was supported by the Foundation for Polish Science (POMOST/2012-6/3 cofunded from POIG 2007–2013). M.Lj.R. and A.R.M. acknowledge support by the MESTD of the Republic of Serbia under Project No. #171020.

Keywords: ab initio calculations · dissociative electron attachment · DNA origami · DNA radiation damage · fludarabine

How to cite: *Angew. Chem. Int. Ed.* **2016**, *55*, 10248–10252
Angew. Chem. **2016**, *128*, 10404–10408

[1] I. Baccarelli, I. Bald, F. A. Gianturco, E. Illenberger, J. Kopyra, *Phys. Rep.* **2011**, *508*, 1–44.
[2] E. Alizadeh, L. Sanche, *Chem. Rev.* **2012**, *112*, 5578–5602.
[3] a) T. Jahnke, H. Sann, T. Havermeier, K. Kreidi, C. Stuck, M. Meckel, M. Schöffler, N. Neumann, R. Wallauer, S. Voss, et al., *Nat. Phys.* **2010**, *6*, 139–142; b) M. Mucke, M. Braune, S. Barth, M. Förstel, T. Lischke, V. Ulrich, T. Arion, U. Becker, A. Bradshaw, U. Hergenhahn, *Nat. Phys.* **2010**, *6*, 143–146.
[4] M. Neustetter, J. Aysina, F. F. da Silva, S. Denifl, *Angew. Chem. Int. Ed.* **2015**, *54*, 9124–9126; *Angew. Chem.* **2015**, *127*, 9252–9255.
[5] B. Boudaiffa, P. Cloutier, D. Hunting, M. A. Huels, L. Sanche, *Science* **2000**, *287*, 1658–1660.
[6] a) T. M. Orlando, D. Oh, Y. Chen, A. B. Aleksandrov, *J. Chem. Phys.* **2008**, *128*, 195102; b) S. V. K. Kumar, T. Pota, D. Peri, A. D. Dongre, B. J. Rao, *J. Chem. Phys.* **2012**, *137*, 045101.
[7] T. Y. Seiwert, J. K. Salama, E. E. Vokes, *Nat. Clin. Pract. Oncol.* **2007**, *4*, 86–100.
[8] a) J. Rak, L. Chomicz, J. Wiczk, K. Westphal, M. Zdrowowicz, P. Wityk, M. Żyndul, S. Makurat, Ł. Golon, *J. Phys. Chem. B* **2015**, *119*, 8227–8238; b) Q.-B. Lu, Q.-R. Zhang, N. Ou, C.-R. Wang, J. Warrington, *EBioMedicine* **2015**, *2*, 544–553; c) R. Schürmann, I. Bald, *J. Phys. Chem. C* **2016**, *120*, 3001–3009.
[9] a) J. Kopyra, C. Koenig-Lehmann, I. Bald, E. Illenberger, *Angew. Chem. Int. Ed.* **2009**, *48*, 7904–7907; *Angew. Chem.* **2009**, *121*, 8044–8047; b) M. Rezaee, E. Alizadeh, P. Cloutier, D. J. Hunting, L. Sanche, *ChemMedChem* **2014**, *9*, 1145–1149.
[10] H. Abdoul-Carime, M. A. Huels, E. Illenberger, L. Sanche, *Int. J. Mass Spectrom.* **2003**, *228*, 703–716.
[11] J. Kopyra, A. Keller, I. Bald, *RSC Adv.* **2014**, *4*, 6825–6829.
[12] F. Ricci, A. Tedeschi, E. Morra, M. Montillo, *Ther. Clin. Risk Manage.* **2009**, *5*, 187–207.
[13] V. Grégoire, N. Hunter, W. A. Brock, L. Milas, W. Plunkett, W. N. Hittelman, *Int. J. Radiat. Oncol. Biol. Phys.* **1994**, *30*, 363–371.
[14] a) P. Swiderek, *Angew. Chem. Int. Ed.* **2006**, *45*, 4056–4059; *Angew. Chem.* **2006**, *118*, 4160–4163; b) I. Bald, I. Dabkowska,

E. Illenberger, *Angew. Chem. Int. Ed.* **2008**, *47*, 8518 – 8520; *Angew. Chem.* **2008**, *120*, 8646 – 8648; c) I. Bald, J. Kopyra, I. Dąbkowska, E. Antonsson, E. Illenberger, *J. Chem. Phys.* **2007**, *126*, 074308; d) J. Kopyra, *Phys. Chem. Chem. Phys.* **2012**, *14*, 8287 – 8289.

[15] A. Keller, I. Bald, A. Rotaru, E. Cauet, K. V. Gothelf, F. Besenbacher, *ACS Nano* **2012**, *6*, 4392 – 4399.

[16] A. Keller, J. Rackwitz, E. Cauet, J. Lievin, T. Körzdörfer, A. Rotaru, K. V. Gothelf, F. Besenbacher, I. Bald, *Sci. Rep.* **2014**, *4*, 7391.

[17] a) A. Keller, J. Kopyra, K. V. Gothelf, I. Bald, *New J. Phys.* **2013**, *15*, 083045; b) S. Vogel, J. Rackwitz, R. Schürman, J. Prinz, A. R. Milosavljević, M. Réfrégiers, A. Giuliani, I. Bald, *J. Phys. Chem. Lett.* **2015**, *6*, 4589 – 4593.

[18] M. A. Huels, B. Boudaïffa, P. Cloutier, D. Hunting, L. Sanche, *J. Am. Chem. Soc.* **2003**, *125*, 4467 – 4477.

[19] M. Rezaee, D. J. Hunting, L. Sanche, *Int. J. Radiat. Oncol. Biol. Phys.* **2013**, *87*, 847 – 853.

[20] a) R. Panajotovic, F. Martin, P. Cloutier, D. Hunting, L. Sanche, *Radiat. Res.* **2006**, *165*, 452 – 459; b) M. Rezaee, P. Cloutier, A. D. Bass, M. Michaud, D. J. Hunting, L. Sanche, *Phys. Rev. E* **2012**, *86*, 031913.

[21] D. Huber, M. Beikircher, S. Denifl, F. Zappa, S. Matejcik, A. Bacher, V. Grill, T. D. Märk, P. Scheier, *J. Chem. Phys.* **2006**, *125*, 084304.

[22] S. Denifl, S. Matejcik, S. Ptasinska, B. Gstir, M. Probst, P. Scheier, E. Illenberger, T. D. Mark, *J. Chem. Phys.* **2004**, *120*, 704 – 709.

[23] F. Kossoski, J. Kopyra, M. T. do N. Varella, *Phys. Chem. Chem. Phys.* **2015**, *17*, 28958 – 28965.

[24] R. Abouaf, J. Pommier, H. Dunet, *Int. J. Mass Spectrom.* **2003**, *226*, 397 – 403.

[25] *CRC Handbook of Chemistry and Physics* (Ed.: D. R. Lide), CRC, Boca Raton, **1992**.

[26] S. Kouass Sahbani, P. Cloutier, A. D. Bass, D. J. Hunting, L. Sanche, *J. Phys. Chem. Lett.* **2015**, *6*, 3911 – 3914.

[27] I. Bald, J. Langer, P. Tegeder, O. Ingólfsson, *Int. J. Mass Spectrom.* **2008**, *277*, 4 – 25.

[28] S. Denifl, P. Sulzer, D. Huber, F. Zappa, M. Probst, T. D. Märk, P. Scheier, N. Injan, J. Limtrakul, R. Abouaf, et al., *Angew. Chem. Int. Ed.* **2007**, *46*, 5238 – 5241; *Angew. Chem.* **2007**, *119*, 5331 – 5334.

[29] H. Abdoul-Carime, J. Langer, M. A. Huels, E. Illenberger, *Eur. Phys. J. D* **2005**, *35*, 399 – 404.

[30] a) T. Sommerfeld, *J. Chem. Phys.* **2007**, *126*, 124301; b) H. Hotop, M.-W. Ruf, M. Allan, I. I. Fabrikant in *Advances in Atomic, Molecular and Optical Physics*, *Vol. 49* (Eds.: B. Bederson, H. Walther), Elsevier, Amsterdam, **2003**.

Received: April 8, 2016
Revised: June 16, 2016
Published online: August 2, 2016

